Reliability-Based Analysis and Life-Cycle Management of Load Tests

Frangopol, Dan M.; Yang, David Y.; Lantsoght, Eva; Steenbergen, Raphaël D.J.M.

Publication date
2019

Document Version
Accepted author manuscript

Published in
Load Testing of Bridges

Chapter 21. Reliability-based analysis and life-cycle management of load tests

Dan M. Frangopol & David Y. Yang

Lehigh University, Bethlehem, PA, USA

Eva O.L. Lantsoght

Politécnico, Universidad San Francisco de Quito, Quito, Ecuador & Concrete Structures, Delft University of Technology, Delft, the Netherlands

Raphaël D.J.M. Steenbergen

TNO, Delft, the Netherlands & Ghent University, Ghent, Belgium

ABSTRACT: This chapter revises concepts related to the uncertainties associated with structures, and how the results of load tests can be used to reduce these uncertainties. When an existing bridge is subjected to a load test, it is known that the capacity of the cross-section is at least equal to the largest load effect that was successfully resisted. As such, the probability density function of the capacity can be truncated after the load test, and the reliability index can be recalculated. These concepts can be applied to determine the required target load for a proof load test to demonstrate that a structure fulfills a certain reliability index. Whereas the available methods focus on member strength and the evaluation of isolated members, a more appropriate approach for structures would be to consider the complete structure in this reliability-based approach. For this purpose, concepts of systems reliability are introduced. It is also interesting to place load testing decisions within the entire life-cycle of a structure. A cost-optimization analysis can be used to determine the optimum time in the life-cycle of the structure to carry out a load test.

1 INTRODUCTION

In this chapter, the effect of load testing on the reliability index is discussed. As the uncertainties play an important role in determining bridge performance, the role of load testing in reducing these uncertainties is an important aspect. The source of the uncertainties can be aleatoric (caused by the inherent randomness of a process) or epistemic (caused by imperfect knowledge) (Ang et al. 2007). The benefit of a successful load test is that the uncertainty associated with the capacity is reduced. Since during a proof load test relatively high loads are applied, which correspond to the factored live loads, the probability density function (PDF) of the

capacity can be truncated after a proof load test at the level of the largest load effect achieved in the test.

The benefit of a diagnostic load test lies in reducing the uncertainties with regard to structural response in terms of, for example, transverse distribution, the effect of bearing restraints, and the contribution of secondary elements like parapets and barriers to the overall stiffness of the structure. A finer assessment can be carried out after a diagnostic load test, and the reliability analysis can be carried out based on the updated finite element model (Gokce et al. 2011). For this approach, no standard procedures have been developed yet. Closely related to the reduction of uncertainties in load tests is also the reduction of uncertainties on the live loads by using Weigh in Motion (WIM) measurements (Casas and Gómez 2013).

The first topic that is discussed in this chapter is the influence of load testing on the reliability index. General concepts related to the determination of the probability of failure and reliability index before, during, and after a proof load test are summarized.

The second topic in this chapter deals with the application of the previously discussed reliability-based concepts to derive the required target proof load to demonstrate a certain reliability index. An example of application is added. This chapter deals with the basic principles of the effect of load testing on the reliability index of a given structure. The analysis of the effects of deterioration are discussed in Chapter 22.

The previously discussed approach deals only with the probabilistic analysis of a structural member. For an evaluation of the entire structure, it is necessary to consider concepts of system reliability. Where direct derivations and research results are not available, possibilities for future research are pointed out.

Zooming out even more brings us to the point of evaluating the structure from the perspective of its life-cycle (Frangopol et al. 1997; Frangopol 2011; Frangopol & Soliman 2016; Frangopol et al. 2017). Cost optimization techniques and time-dependent effect such as material degradation and deterioration can be used to evaluate which point in time during the life-cycle of the structure would be the optimal moment for load testing and assessing the structure (Frangopol & Liu 2007; Okasha & Frangopol 2009; Barone & Frangopol 2014a; Sabatino et al. 2015; Kim & Frangopol 2017). These concepts fit in the philosophy of using life-cycle analysis to determine the optimal time for maintenance, repair, rehabilitation, and inspection of a given structure. An even further step would be to consider the bridge structure as part of an infrastructure network, and determine the optimum point in time for load testing the structure based on a cost-optimization that balances the economic, environmental, and social costs of the load test and benefits

from the perspective of the entire infrastructure network (Liu & Frangopol 2005; Liu & Frangopol 2006a; Liu & Frangopol 2006b; Bocchini & Frangopol 2011; Bocchini & Frangopol 2012; Bocchini & Frangopol 2013; Dong et al. 2015).

2 INFLUENCE OF LOAD TESTING ON RELIABILITY INDEX

2.1 General principles

To determine the probability of failure P_f, the distribution functions of the resistance R and the loading S are necessary. Resistance or load effect can be approximated by different probability distributions. Examples of such well-defined distribution functions are: uniform distribution, normal distribution, lognormal distribution, and extreme value distribution, among others. The mathematical expression of these distributions can be consulted in textbooks (Melchers 1999). For structural engineering applications, recommendations for the choice of the type of distribution functions and governing parameters of the selected distribution functions are given in the JCSS Probabilistic Model Code (JCSS 2001b). These recommendations, however, do not differentiate between newly designed structures and existing structures.

The next step in determining the probability of failure, is the determination of the limit state function g. For structural applications, the limit state function g can be taken as the difference between the resistance R and the loading S:

$$g = R - S \tag{1}$$

When $g < 0$, the resistance is smaller than the applied loading, and failure occurs. The chance that $g < 0$ is called the probability of failure, P_f. This probability of failure P_f can be translated into the reliability index β:

$$\beta = \Phi^{-1}\left(1 - P_f\right) \tag{2}$$

where Φ^{-1} is the inverse normal distribution. Current design codes and codes for assessment have derived load and resistance factors based on a minimum required reliability index (target reliability index).

The expression of the probability of failure before the load test, P_{fb}, as shown in Figure 1a, is expressed based on the following convolution integral:

$$P_{fb} = \int_{-\infty}^{+\infty} \left(1 - F_s\left(r\right)\right) f_R\left(r\right) dr \tag{3}$$

In Equation (3), $F_s(r)$ is the cumulative distribution function (CDF) of the loading S and $f_R(r)$ is the probability density function (PDF) of the resistance R.

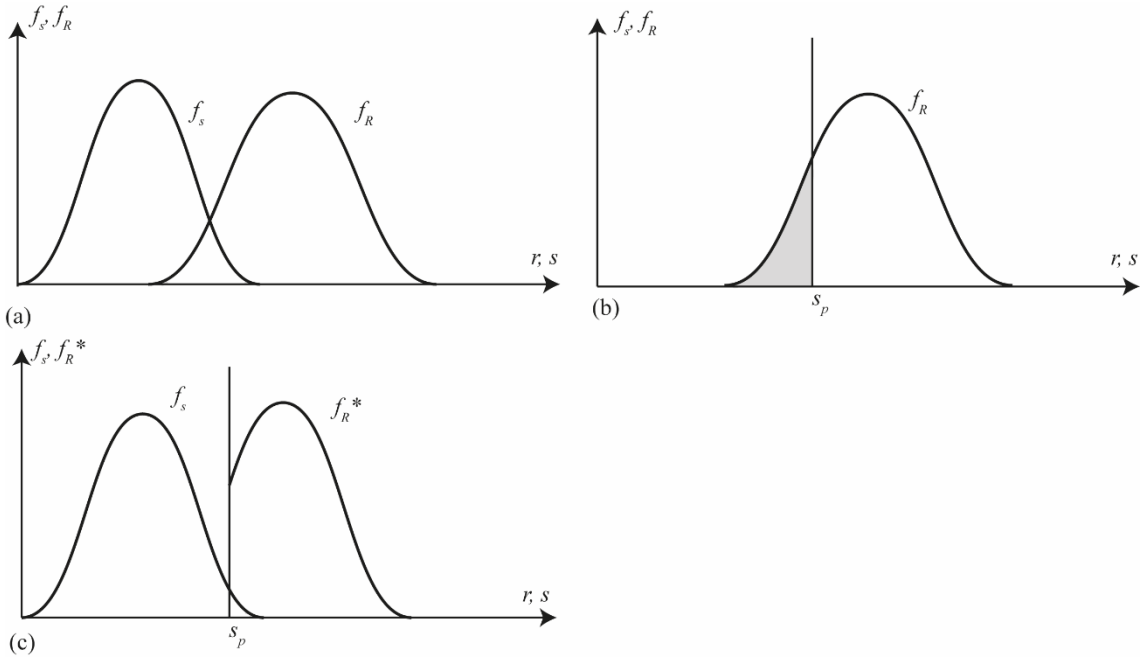

Figure 1: Determination of the probability of failure: (a) before, (b) during, and (c) after a load test during which the target proof load s_p was applied. Highlighted region shows the probability of failure in figure 1(b). Figure from (Lantsoght et al. 2017c). Reprinted with permission.

During a load test, the loading and resulting load effect S are not a random variable, but a deterministic value of the applied load s_p. The distribution function of the loading, f_s, is thus replaced by the deterministic value s_p as shown in Figure 1b. The probability of failure during the test, P_{fd}, is described by the cumulative distribution function (CDF) of the resistance F_R:

$$P_{fd} = F_R\left(s_p\right) \tag{4}$$

After a successful load test, it is known that the resistance is at least equal to the maximum load effect that was achieved during the test, provided that no signs of distress were observed. The convolution integral from Equation (3) can be updated with the information that is obtained during the load test. As a result, the PDF of the resistance, f_R, can be updated into a truncated distribution function f_R^*, as shown in Figure 1c. The probability of failure after the load test, updated with the information from this test, P_{fa}, is then determined as

$$P_{fa} = \frac{1}{1-F_R\left(s_p\right)} \int_{s_p}^{+\infty} \left(1-F_s\left(r\right)\right) f_R\left(r\right) dr \tag{5}$$

The presented values for the probability of failure before, during, and after a load test are valid provided that there is no correlation between R and S. Solutions for cases where R and S are correlated, or for structures with quality problems are available in the literature (Spaethe 1994).

The previous considerations for P_{fa}, for which the value of P_{fa} is larger than P_{fb} as a result of the load test, are only valid for a successful load test. Another possible outcome of a load test is that P_{fa} is smaller than P_{fb}. This case occurs after a load test during which a stop criterion is exceeded. Exceeding a stop criterion means that further loading will result in irreversible damage to the structure or even collapse. As such, the load for which a stop criterion is reached can be considered the lower bound of the structural capacity. The outcome of the load test is then that a deterministic value of the capacity is found as the load effect caused by the load s_s for which a stop criterion is exceeded. When a stop criterion is exceeded during a load test, the probability of failure during the test $P_{fd} = 1$ with $s_s < s_p$, see Figure 2b. The probability of failure after the load test P_{fa} can then be calculated as:

$$P_{fa} = 1 - F_S(s_s) \tag{6}$$

where F_S the CDF of the load effect and s_s the load for which a stop criterion is exceeded, as shown in Figure 2c. The result is then that the reliability index after the test β_a is lower than that before the test β_b.

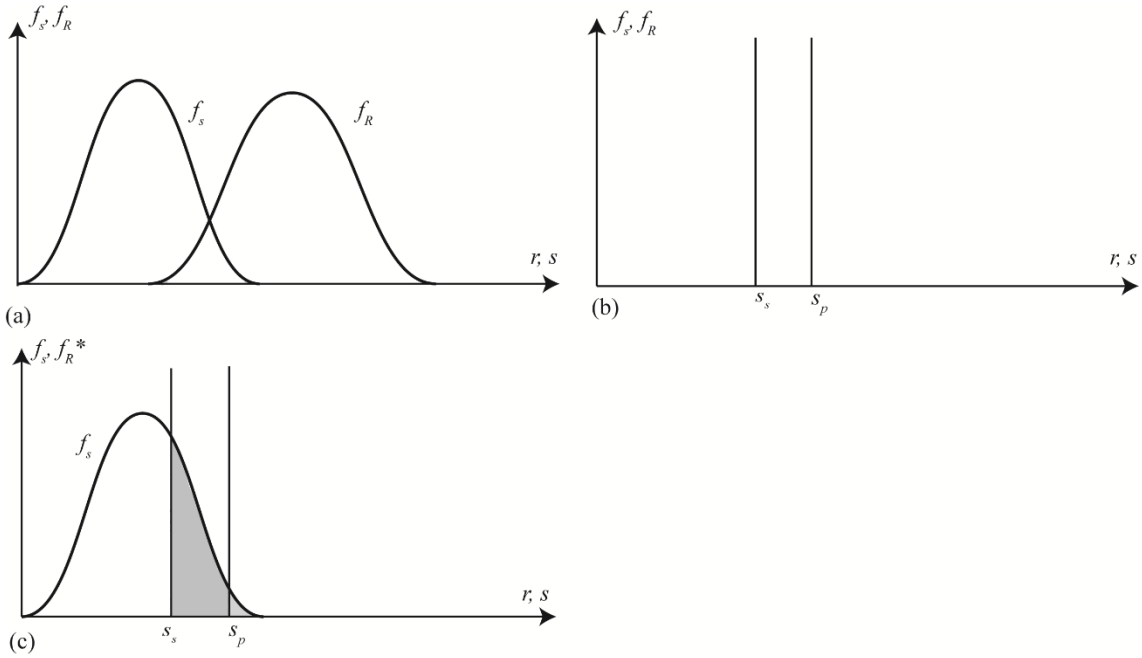

Figure 2: Determination of the probability of failure: (a) before, (b) during, and (c) after a load test during which a stop criterion was exceeded for s_s. Highlighted region shows the probability of failure.

The magnitude of the load before (s_k), during (s_p), and after the load test (s_k) is shown in Figure 3a. The figure also shows the possibility for an increase of the loads with a factor ξ_p over time as a result of changes in traffic loads and intensities, for example when a heavier truck type is permitted circulation. Figure 3a reflects the fact that in proof load tests loads (s_p) are used that are higher than the characteristic live loads. The effect on the reliability index before, β_b, during, β_d, and after, β_a, a load test is shown in Figure 3b for the case when the target proof load s_p is applied and in Figure 3c for the case when a stop criterion is exceeded at s_s prior to reaching s_p. The value of β_b can be quantified with Eq. (3). The value of β_d for a load test in which s_p is applied is quantified with Eq. (4) and $\beta_d = 0$ when a stop criterion is reached at a load s_s. The value of β_a for a load test during which s_p is applied can be quantified according to Eq. (5) and for a load test terminated at s_s according to Eq. (6). If the applied target load s_p is large enough, the updated information after the test will result in a larger reliability index β_a after the load test than β_b before the load test. Since during the load test a higher load s_p is used than the characteristic live load s_k, the reliability index temporarily drops to β_d during the load test. If a stop criterion is exceeded during the test and a load s_s lower than s_p is applied, the lower bound for failure is found during the test, β_d becomes zero, and the value of β_a will be lower than β_b.

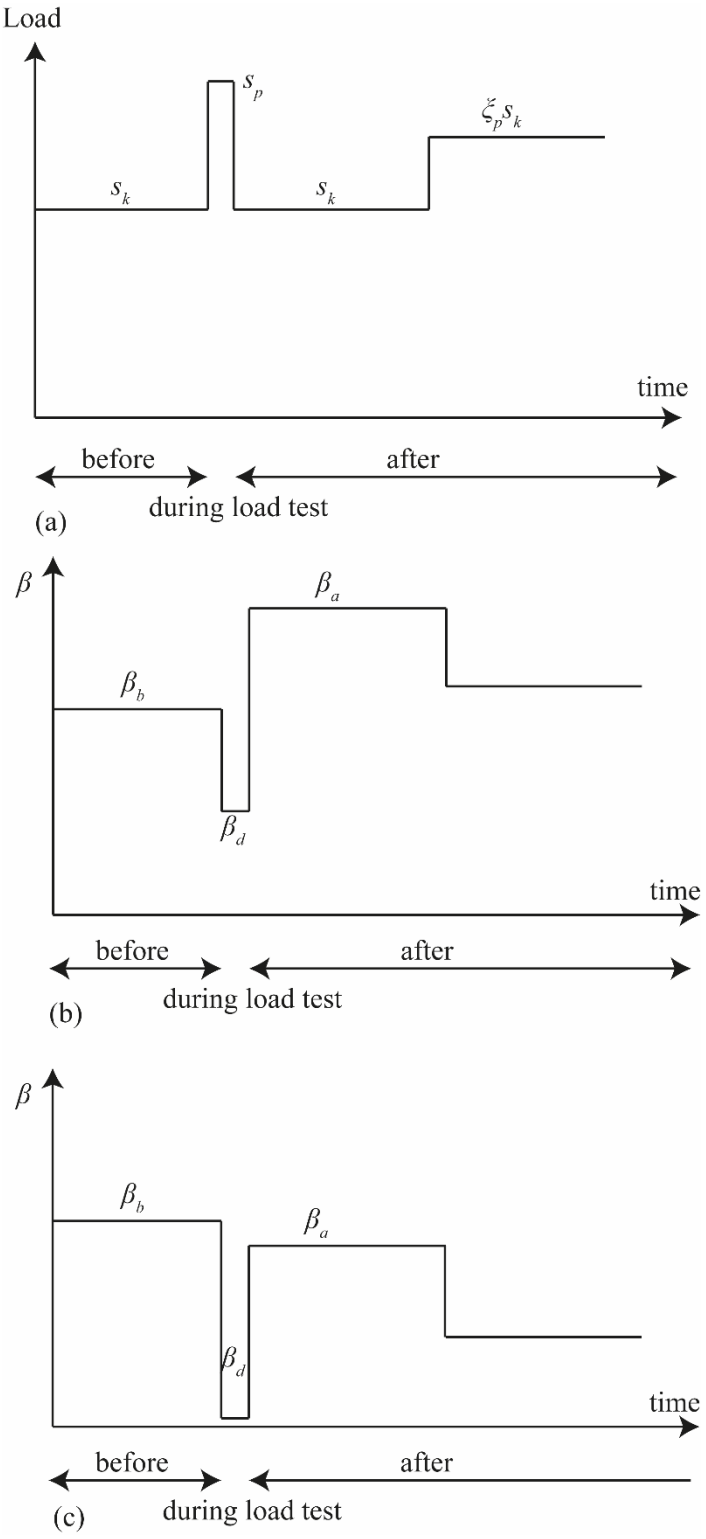

Figure 3: Change of reliability index before β_b, during β_d, and after load test β_a, based on (Spaethe 1994): (a) value of the load before (s_k), during (s_p), and after load test (s_k), including the effect for future increases in load with a factor ξ_p; (b) effect on reliability index before, during, and after load test when s_p is applied; (c) effect on reliability index before, during, and after load test when the test is terminated at s_s.

2.2 **Effect of degradation**

The effect of degradation is discussed in more detail in Chapter 22. Here, only a few basic concepts are reviewed. The concepts shown in Figure 3 do not take into account the effect of degradation. The resistance R decreases over time as a result of material degradation and deterioration. For computations, the probability density function (PDF) of the resistance f_R and the cumulative distribution function (CDF) F_R can be expressed as a function of the time t. The limit state function then becomes time-dependent (Frangopol and Kim 2014). Degradation increases the probability of failure over time and decreases the reliability index over time. The effect of this reduction of the reliability index is shown in Figure 4a for a load test in which s_p was applied and in Figure 4b for a load test terminated at s_s.

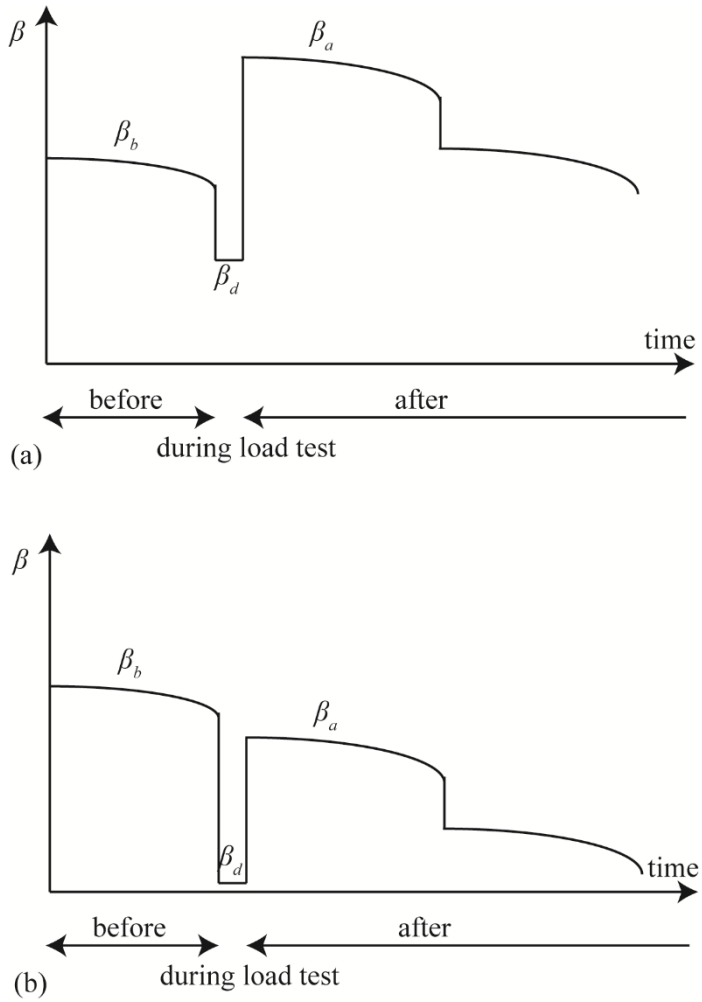

Figure 4: Change of reliability index before β_b, during β_d, and after load test β_a, for applied loads shown in Figure 3a and taking into account degradation (a) effect on reliability index before, during, and after load test when s_p is applied; (b) effect on reliability index before, during, and after load test when the test is terminated at s_s.

For concrete bridges, the main inducer of service life reduction is corrosion of the reinforcement. Corrosion can affect both flexural reliability and shear reliability (Enright and Frangopol 1998, Vatteri et al. 2016). Corrosion also reduces the probability of exceeding the serviceability requirements (Li et al. 2005).

For steel bridges, fatigue and fracture can cause structural failure. The results from inspections can be used to update estimates of the remaining service life by improving the calibration of the probabilistic degradation model (Righiniotis and Chryssanthopoulos 2003). The failure probability is then determined based on conditional probabilities (Lukic and Cremona 2001, Zhu and Frangopol 2013).

The idea of updating the effect of degradation after inspections can also be applied to load testing. The information from a load test can be used to update the estimate of the remaining service life. The concepts from updating the estimated service life based on data from structural health monitoring (Messervey & Frangopol 2008; Messervey 2009; Messervey et al. 2011) can be applied. The use of load testing data to update the estimate of the remaining service life is a topic that needs further research.

2.3 Target reliability index and applied loads

For existing structures, the target reliability index is lower than that of a structure in the design stage (Stewart et al. 2001, Steenbergen and Vrouwenvelder 2010). The following factors determine the target reliability index for assessment: consequences of failure, reference period, remaining service life, relative cost of safety, and importance of the structure. When the maintenance and repair costs are large, and the consequences of failure are minor, lower reliability indices are tolerated as assessment result. These values result from a cost optimization that considers the structural cost, the cost of damage, and the probability of failure, see Figure 5. For the loss of human life, a lower bound of $\beta = 2.5$ with a reference period of one year (Steenbergen and Vrouwenvelder 2010) should be considered.

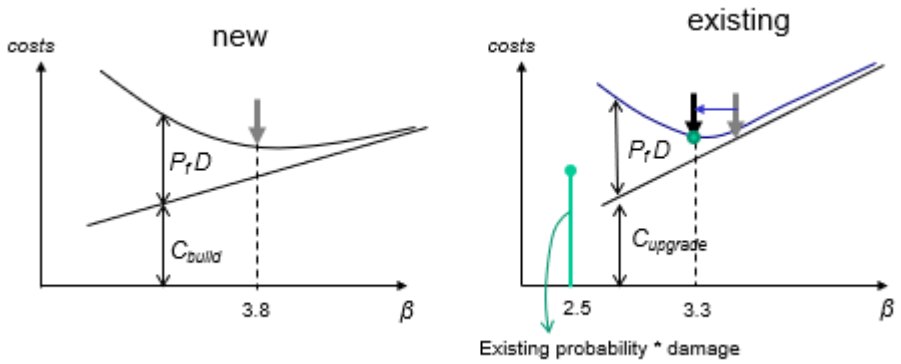

Figure 5: Resulting target reliability index after cost-optimization.

Stewart et al. (Stewart et al. 2001) suggest a target reliability index for a one year reference period between 3.1 and 4.7. Target reliability indices have also been suggested as a function of the age of the bridge and its remaining lifetime (Koteš and Vican 2013), resulting in target indices between 2.692 (for a bridge of 90 years with a remaining lifetime of 2 years) and 3.773 (for a bridge of 10 years with a remaining lifetime of 90 years).

In Europe, the factored live load model is used (Olaszek et al. 2012) for proof load tests, and a target proof load is then applied that creates the same sectional shear or moment as the factored live load model. When the factored live load model is used to find the target proof load, it is tacitly assumed that the resulting reliability index and probability of failure after the test (if the test is successful) of the bridge have the same value as what the load factors are calibrated for.

In the Netherlands, target reliability indices and load factors have been formulated for existing structures in the Dutch Code NEN 8700:2011 (Code Committee 351001 2011). The application to highway bridges is provided in the guidelines for the assessment of bridges RBK (Rijkswaterstaat 2013), and prescribes reliability indices between 3.1 (with a reference period of 15 years) and 3.6 (with a reference period of 30 years). In the United States, a target reliability index of 2.3 (with a reference period of 5 years (Šavor and Šavor Novak 2015)) was determined for rating at the operating level, and for rating at the inventory level a reliability index of 3.5 (for a lifetime reference period of 75 years (Šavor and Šavor Novak 2015)) (NCHRP 1998).

3 REQUIRED TARGET LOAD FOR UPDATING RELIABILITY INDEX

3.1 **Principles**

The general expression for the limit state function is given in Equation (1). Depending on the goal of the load test, the expression for the limit state function can be expressed based on the failure mode that needs to be evaluated. For concrete bridges, typically bending moment and shear are evaluated, and the governing failure mode is further studied. For bending moment, the following limit state violation is found:

$$g = m_R - m_S < 0 \tag{7}$$

This limit state is expressed based on the bending moment capacity m_R and the sectional moment caused by the applied loads m_S, where m_R and m_S are random variables.

For shear, the following limit state violation can be used:

$$g = v_R - v_S < 0 \tag{8}$$

where v_R the shear capacity of the cross-section under consideration and v_S the shear stress caused by the applied loads, with v_R and v_S random variables.

In order to determine the probability of failure, the distribution functions need to be determined. There are different approaches to determine the distribution functions of m_R, m_S, v_R and v_S. When no information about the actual traffic is available and no distribution function of the live loads can be extrapolated from WIM measurements (Obrien et al. 2015), the load combination using the load model from the code is used. Another possibility, when no information about the actual traffic is available, is to take the traffic load models from *fib* Bulletin 80 (fib Task Group 3.1 2016). In the case of a bridge-specific traffic load model, it is advised to use Monte Carlo simulation of traffic flow using WIM data over influence lines or fields of the bridge sections under consideration. Here appropriate values for the statistical and model uncertainty should be taken into account. The distribution function of the resistance can be determined considering aleatory uncertainties of material properties and epistemic uncertainties of structural models. The Probabilistic Model Code (Joint Committee on Structural Safety 2001) can be used as a starting point to select the shape of the distribution function, the bias, and the coefficient of variation. However, this code makes no distinction between newly designed structures and existing structures that need to be assessed.

3.2 **Example: Viaduct De Beek – Information about traffic is not available**

3.2.1 *Description of Viaduct De Beek*

Viaduct De Beek, see Figure 6, (Lantsoght et al. 2017a, Lantsoght et al. 2017d) is a reinforced concrete slab bridge over highway A67 in the province of Noord Brabant in the Netherlands. It has been in service since 1963. In 2015, the conclusion of an assessment was that posting or restricting the use of the viaduct is necessary (Willems et al. 2015), because the flexural capacity of the viaduct is insufficient. As a result, the use of the viaduct was restricted from two lanes to one lane, see Figure 6b.

Figure 6: Viaduct De Beek (a) side view; (b) traffic restriction.

The geometry of viaduct De Beek is shown in Figure 7. The viaduct has four spans: two end spans with a length of 10.81 m (35.5 ft) and two central spans with a length of 15.40 m (50.5 ft). The total width is 9.94 m (32.6 ft), and the carriageway is 7.44 m (24.4 ft) wide, which facilitates two lanes of 3.5 m (11.5 m) width each way. Since 2015, the traffic restriction results in only one lane, which is facilitated by the use of barriers. The profile is parabolic in the longitudinal direction and varies from 470 mm (18.5 in) to 870 mm (34.3 in) (see Figure 7b).

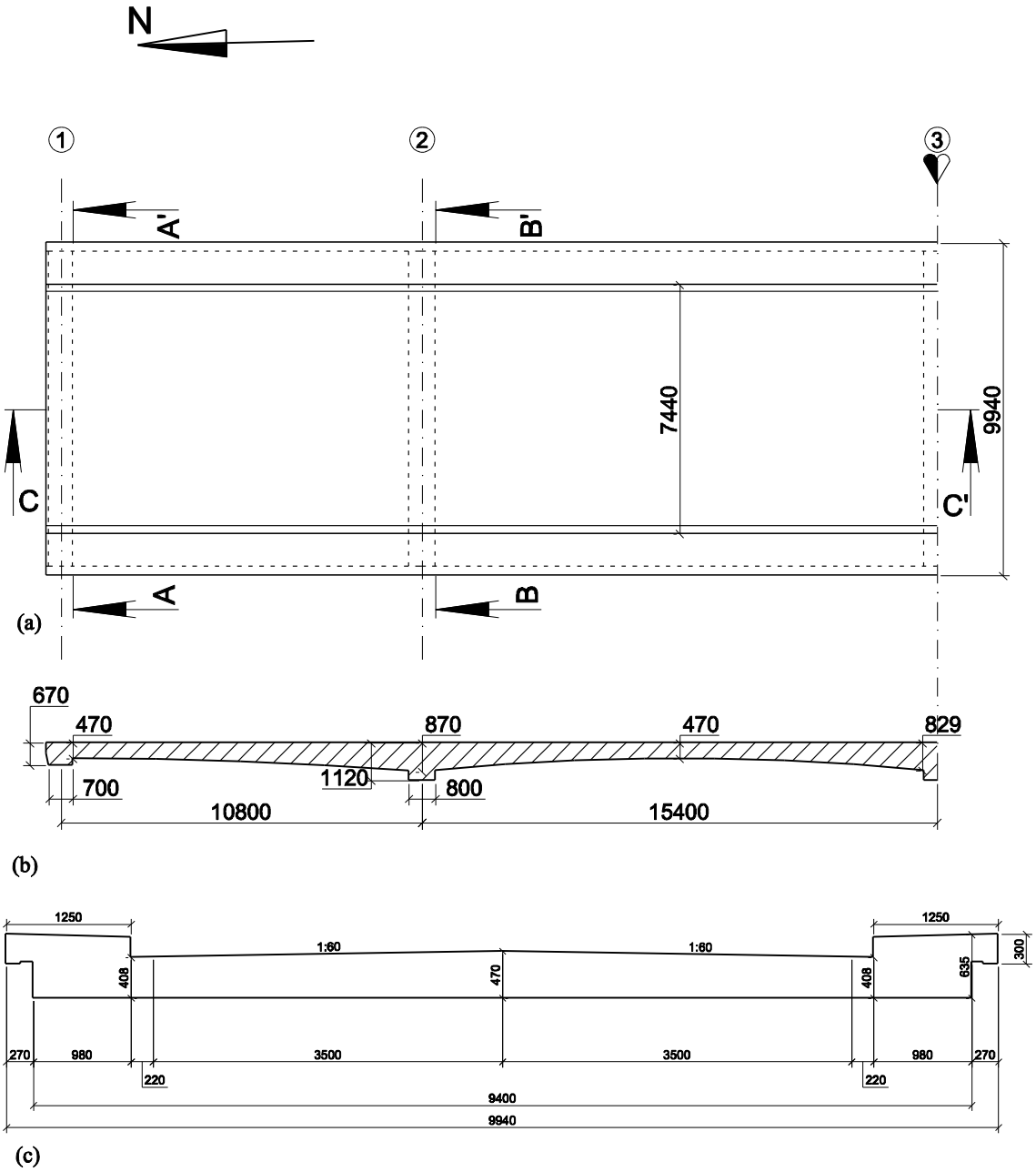

Figure 7: Geometry of viaduct De Beek: (a) top view; (b): side view at section C-C'; (c) cross-section at section A-A' (Lantsoght et al. 2017d), reprinted with permission. Dimensions in mm. Conversion: 1 mm = 0.04 in.

The concrete compressive strength was determined based on core samples. The characteristic concrete compressive strength was determined as f_{ck} = 44.5 MPa (6.5 ksi), and the design compressive strength was found as f_{cd} = 30 MPa (4.4 ksi). The properties of the steel were determined by sampling. It was found that the average yield strength of the steel was f_{ym} = 291 MPa (42.2 ksi), the tensile strength of f_{tm} = 420 MPa (60.9 ksi), and that the design yield strength can be assumed as f_{yd} = 252 MPa (36.6 ksi). Plain reinforcement bars were used. The reinforcement layout is shown in Figure 8. The thickness of the asphalt layer was measured on core samples to lie between 50 mm (2.0 in) and 75 mm (3.0 in).

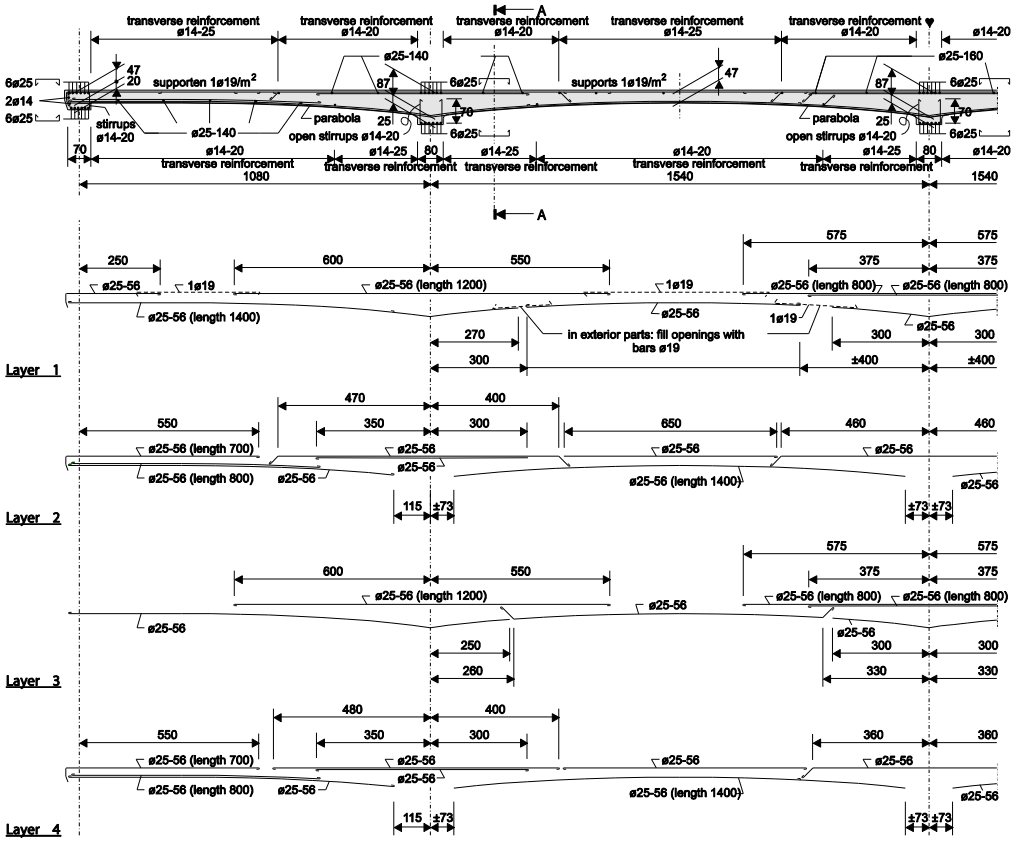

Figure 8: Reinforcement layout of Viaduct De Beek. Reprinted with permission from ASCE from (Lantsoght et al. 2017b).

At the Dutch RBK Usage level (load factors derived for β = 3.3 for a reference period of 30 years) (Rijkswaterstaat 2013), the Unity Check (ratio of factored acting moment to factored moment capacity) is determined as UC = 1.02 in the governing section and at the Eurocode ULS level (load factors derived for β = 4.3 for a reference period of 100 years), the maximum value is UC = 1.10. Since the Unity Checks are larger than 1, the assessment indicates that the section does not fulfill the requirements for the Eurocode ULS level based on an analytical assessment.

This assessment is carried out by using a linear finite element model in which the load combination of the self-weight, superimposed dead load, and live loads from NEN-EN 1991-2:2003 (CEN 2003) are applied. For shear, the Unity Check at the RBK Usage level is UC = 0.48, so that the failure mode of shear will not be further studied, as the bridge fulfills the requirements for shear for all safety levels. To verify if viaduct De Beek can carry the code-prescribed live loads for bending moment, a load test was carried out to assess the bridge.

A limitation for the execution of the proof load test on viaduct De Beek was that only the first span could be tested. Testing the more critical second or third spans was not allowed, as these spans are above the highway. To safely test these spans, the highway would have to be closed, which was not permitted by the road authority.

3.2.2 *Determination of required target load*

Based on a traditional approach, as described in Chapter 13, the required proof load for bending moment and shear, applied on a single design tandem, are as given in Table 1. In this approach, the target proof load is determined as the load that results in the same sectional moment or shear as the factored load combination. For research purposes, the shear-critical position was also tested. These results are not discussed here. For more information about these results, please refer to (Lantsoght et al. 2017a). The maximum load that was applied during the bending moment test was 1751 kN (394 kip) (including the weight of the equipment), which corresponds to the Eurocode ULS safety level, plus 6% extra.

Table 1: Required proof load for bending $P_{load,bending}$ as determined based on the traditional approach for the different safety levels. Conversion: 1 kN = 0.225 kip.

Safety level	$P_{load,bending}$ (kN)
Eurocode Ultimate Limit State	1656
RBK Design	1649
RBK Reconstruction	1427
RBK Usage	1373
RBK Disapproval	1369
Eurocode Serviceability Limit State	1070

To determine the target proof load based on the principles outlined before, the solution for Equation (5) in terms of s_p is sought that corresponds to the target reliability index β_a that needs to be proven with the applied proof load. The reliability index that is associated with each safety level used in the Netherlands is indicated in Table 2. In a proof load test, the probabilistic influence factor α_S for stochastic considerations with proof load testing can be taken as $\alpha_S = 0.8$. The target reliability indices that would result after a proof load test are then given in Table 2 as $\alpha\beta$.

Table 2: Considered safety levels, and reliability index and reference period associated with the load factors of the considered safety level.

Safety level	β	Reference period	$\alpha\beta$
Eurocode Ultimate Limit State	4.3	100 years	3.44
RBK Design	4.3	100 years	3.44
RBK Reconstruction	3.6	30 years	2.88
RBK Usage	3.3	30 years	2.64
RBK Disapproval	3.1	15 years	2.48
Eurocode Serviceability Limit State	1.5	50 years	1.20

Since no information about the traffic on the bridge is available, the analysis is carried out based on the bending moment capacity m_R and the occurring bending moment m_S caused by the load combination of the code. This load combination consists of the self-weight, the superimposed dead load, and the live loads consisting of a design truck in both lanes and the distributed live loads. It is necessary to consider the live loads in both lanes if the goal of the proof load test is to remove the current traffic restrictions. The bending moment m_S was determined by using a linear finite element model. The average value of the acting bending moment is determined by using all load factors as equal to 1, and results in m_S = 385 kNm/m (87 kip-ft/ft). The average value of the bending moment resistance is determined based on the mean values of the material parameters and is m_R = 673 kNm/m (151 kip-ft/ft).

To develop the probability density functions of the acting bending moment and the bending moment resistance, the recommendations of the JCSS Probabilistic Model Code (JCSS 2001b) are followed. The shape of the functions is recommended to be lognormal. The recommendation for the bending moment resistance includes a mean of 1.2 and a coefficient of variation of 0.15.

For the acting bending moment, the case of moments in plates is selected, for which the recommendations are to use a mean of 1.0 and a coefficient of variation of 20%. The resulting probability density functions are shown in Figure 9.

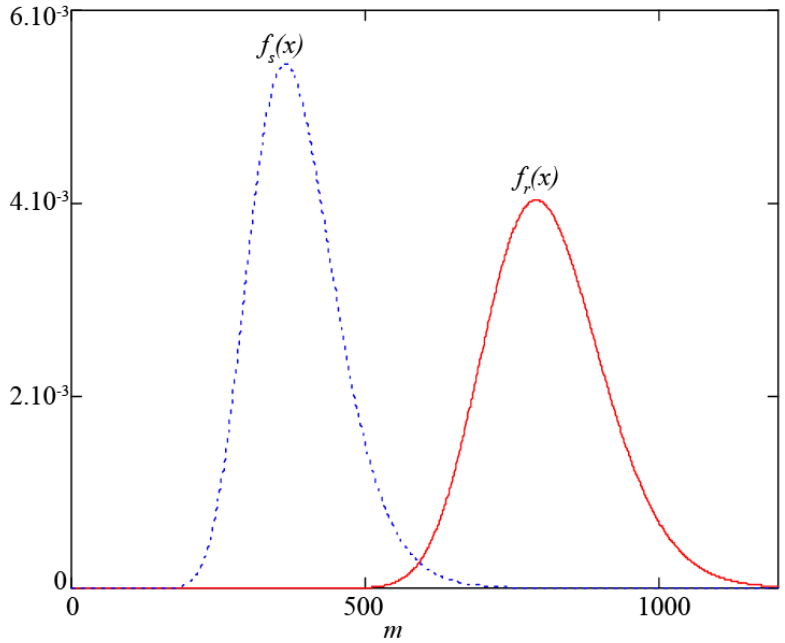

Figure 9: Resulting probability density functions for the acting bending moment m_s and the bending moment resistance m_R.

The solution of Equation (3) for the PDFs in Figure 9 gives the reliability index prior to the proof load test, which equals $\beta_b = 3.02$. Considering this result, it would not be interesting to proof load test for any other safety level than the RBK Design level. The reliability index prior to load testing was $\beta_b = 3.02$. The goal of a proof load test is to increase this value. It can be seen in Table 2 that only the RBK Design level has a value of $\alpha\beta$ that is larger than 3.02, which is 3.44.

In a next step, the target proof load s_p is determined so that after the proof load test the requirements of the RBK Design safety level are fulfilled. The value of $\alpha\beta$ for this safety level can be read from Table 2 as 3.44. As such, the value of s_p is sought that results in a reliability index after proof load testing of $\beta_a = 3.44$. The required value to find $\beta_a = 3.44$ is a load that causes a bending moment of 655 kNm/m (147 kip-ft/ft). Reverse analysis then was used to determine that this load equals 1951 kN (439 kip). This required load is significantly larger than the load found by using the traditional approach. This result shows that when a certain reliability index needs to be proven during a proof load test, high loads are required. These high loads increase the risks for the personnel, structure, and traveling public during the test.

3.2.3 *Discussion of results*

The fact that the required load of 1951 kN (439 kip) for proving the target reliability index of 3.44 is larger than the load found with the traditional approach as 1656 kN (372 kip) can be explained by three reasons. The first reason is that no information about the traffic distribution is taken into account for this example. This reason is mitigated by the next example. The second reason is that the recommendations for developing the probability density function from the JCSS Probabilistic Model Code (JCSS 2001b) prescribe rather large coefficients of variation. The third reason is that the recommendations from the JCSS Probabilistic Model Code (JCSS 2001b) are general recommendations, and that these recommendations may need to be altered for the particularities related to existing structures.

A sensitivity analysis of the assumptions from the JCSS Probabilistic Model Code (JCSS 2001b) was carried out (Lantsoght et al. 2017c). The value of the coefficient of variation on the bending moment resistance m_R was varied between 5% and 15%. It can be argued that is coefficient of variation can be reduced from the recommended value of 15%, since the only variable is the yield strength of the steel. For modern steel types (JCSS 2001b, Karmazinova and Melcher 2012) the coefficient of variation of the yield strength of the steel is 7%. However, this value may not be representative of the variation on the steel that was used in the past and that can be found in many existing bridges. Data and recommendations for historically used rebar steel types in the Netherlands are not available. In the sensitivity analysis, a mean value of both 1.2 and of 1.0 was used for m_R. Additionally, the value of the coefficient of variation on the acting bending moment m_s was varied between 5% and the recommended value of 20%. The recommended value for moments in plates of a coefficient of variation of 20% can be considered rather large, and is significantly larger than the coefficient of variation of 5% for stresses in 3D models recommended by the JCSS Probabilistic Model Code. Therefore, this range of values was studied in the sensitivity analysis.

With the aforementioned ranges for the coefficients of variation of the acting bending moment and the bending moment capacity and for the mean value of the bending moment capacity, the convolution integrals of Equations (3), (4), and (5) are solved. The applied load during the proof load test is taken for all cases as 1751 kN (394 kip), the maximum load that was applied in the field. This load results in a bending moment of 597 kNm/m (134 kip-ft/ft), which is used for the value of s_p. In the sensitivity analyses it is found that the resulting reliability index after testing β_a varies between 2.85 and 6.66. This analysis thus shows that uniform recommendations for the required coefficient of variation need to be developed that are applicable to proof load testing and existing structures, so that a simplified reliability-based approach can be used for the

determination of the target proof load for bridges where no WIM data are available. It must be noted here as well that the effect of carrying out the proof load test becomes smaller as the coefficients of variation (and thus, the uncertainties) are reduced. Another discussion that should be held is whether proof load tests should have as a goal to demonstrate a certain reliability index and probability of failure for a bridge, or if it is sufficient to know that a certain type of vehicle can pass safely, taking a safety margin based on a simple magnification factor as used in the Manual for Bridge Evaluation (AASHTO 2016), into account.

3.3 **Example: Halvemaans Bridge – Information about traffic is modeled**

3.3.1 *Description of Halvemaans Bridge*

The Halvemaans Bridge, see Figure 10, (Fennis and Hordijk 2014) is a single-span reinforced concrete slab bridge in the city of Alkmaar in the Netherlands. The bridge has been in service since 1939. An assessment led to the conclusion that the bridge does not fulfil the code requirements for bending moment when subjected to live Load Model 1 of NEN-EN 1991-2:2003 (CEN 2003). The Halvemaans Bridge was subjected to a proof load test in the spring of 2014.

The geometry of the Halvemaans Bridge is shown in Figure 11. The span length is 8.2 m (27 ft) and the slab has a skew angle of 22^{o}. The total width is 7.5 m (25 ft) and the carriageway width is 5.5 m (18 ft), see Figure 12. The thickness of the concrete deck is 450 mm (18 in) and the thickness is increased to 590 mm (23 in) at the sides, see Figure 12. The abutments are masonry walls with a thickness of 0.33 m (1 ft). Details of the reinforcement layout are given in Figure 12. It is assumed that the reinforcement lies parallel to the axis of the bridge. No core samples were taken to determine the concrete compressive strength, which was estimated to be f_{cm} = 68 MPa (9863 psi).

Figure 10. Halvemaans Bridge.

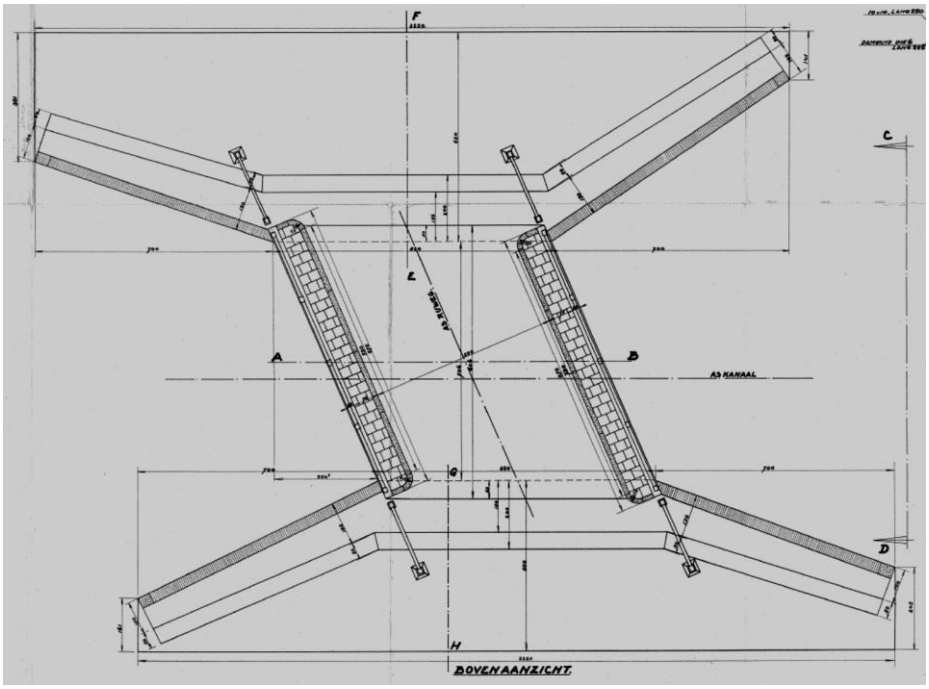

Figure 11. Geometry of Halvemaans Bridge, top view.

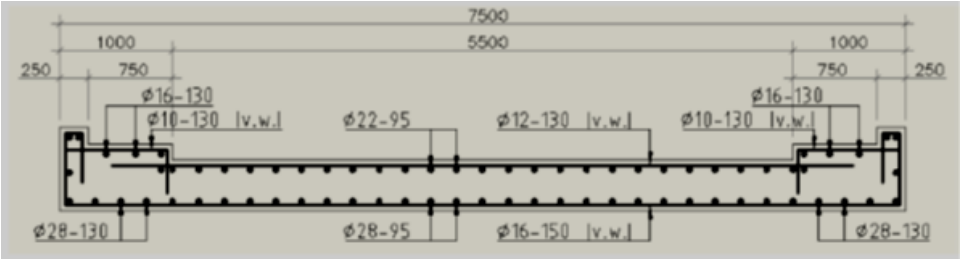

Figure 12. Cross-section of Halvemaans Bridge.

3.3.2 *Determination of proof load*

In the analysis for the determination of the exact value of the proof loading the following aspects were taken into account. In these aspects the determination of the proof load differs from the determination of the 'normal' design load for a bridge assessment using models and building codes.

1. In the event of a proof loading, the bridge is deterministically loaded by its self-weight, so there is no uncertainty about it. For the permanent action for this bridge it is assumed that it will not change in the future. As a result, the contribution of the permanent load to the failure probability will be zero and need not be included in the proof loading value.

2. It is clear that, if the bridge is proof loaded to its ultimate capacity, there is no uncertainty about the strength either. In a probabilistic analysis (the basis of the proof loading determination) all uncertainty will be on the load side. This means that from that perspective the load factor during proof loads is significantly larger than normally used for calculations. Differently formulated, for the loads S the probabilistic influence factor α_S is usually taken as 0.7 (ISO 2394 (ISO/TC 98/SC 2 Reliability of structures 2015) and NEN-EN 1990:2002 (CEN 2002)); in the case of a proof load α_S should be increased from 0.7 to 1.0, if through the proof loading we get to know the resistance R exactly. However, through proof loading, in general, we know that the real capacity is larger than the capacity needed to carry the proof loading. This leads to an increase in α_S. In this case α_S =0.8 was assumed.

3. The model uncertainty (JCSS 2001a), representing the uncertainty in the load effect calculation will be smaller than normally used. Using proof loading namely, in general less calculations are done. This reduces the load factor if compared to normal structural calculations.

In Figure 13, the complementary cumulative distribution function of the daily maxima of the traffic load effects is shown; it has been generated using the influence lines of the bending moment in the mid span of the bridge. Way in Motion (WIM) data is used to sample the traffic flow. The red line gives the empirical distribution function; the blue line is the fitted analytical distributed function which is used in the full probabilistic analysis for the determination of the proof loading value. The WIM measurements result from a bridge subjected to 2.5 million trucks per year. Since the Halvemaans Bridge is subjected to only 51,500 trucks per year, this difference is corrected for in the distribution function of the traffic load effect. Statistical uncertainty was included to account for the uncertainty in the extrapolated part of the distribution function.

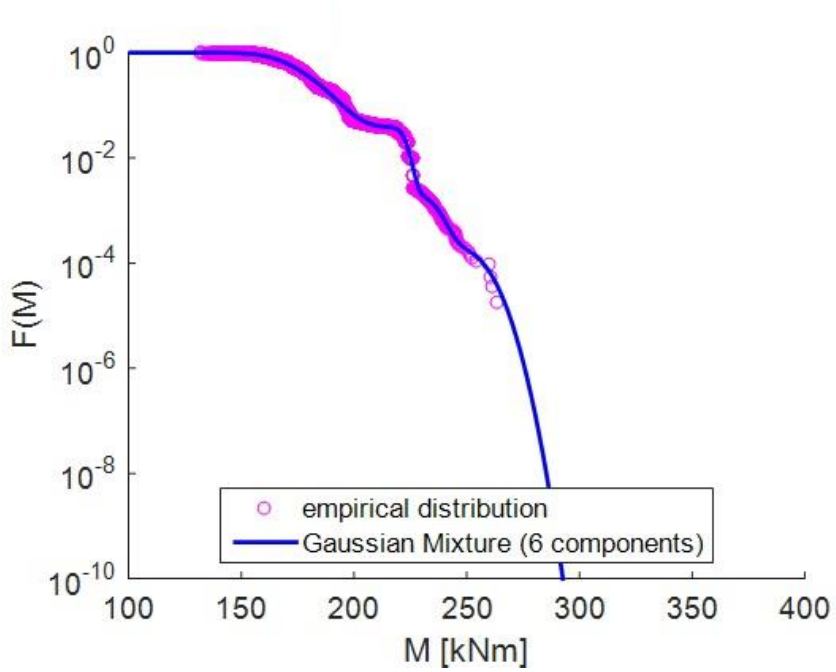

Figure 13. Distribution of the daily maxima of the simulated traffic load effect.

The proof load that is applied to the Halvemaans Bridge in the field is distributed load over the width of one lane (3 m = 9.8 ft wide) instead of over four wheel prints to facilitate execution. With this proof load, it should be demonstrated that the requirements of the repair level for Consequences Class 2 of NEN 8700:2011 (Code Committee 351001 2011) are fulfilled, namely a reliability index $\beta = 3.1$ for a reference period of 15 years. Using the reduction factor $\alpha_S = 0.8$ gives a target reliability index of $\alpha_S\beta = 2.5$ (reference period 15 years). The WIM measurements are used for simulations for a simply supported wide beam (representing the slab bridge) of 7 m (23 ft) length. The resulting bending moment at mid-span of the bridge is translated into a distributed load q_{EUDL} over the entire span length. Probabilistic calculations showed that a load of

q_{EUDL} = 175 kN/m (12 kip/ft), or a load that causes the same sectional moment at midspan in the bridge, should be applied during a proof load test. The proof load that causes the same sectional moment at midspan of the bridge is found to be 85 ton (94 short tons). The maximum load that was ultimately applied during the proof load test was 90 ton (99 short tons), which resulted in the conclusion that, based on the current knowledge regarding the interpretation of proof load test results for structural safety, the bridge fulfils the code requirements for CC2 at the repair level.

4 SYSTEMS RELIABILITY CONSIDERATIONS

A bridge structure is comprised of various structural elements. The method described previously is mainly focused on element reliability. In order to ensure the safety of the entire bridge, system reliability analyses should be conducted (Frangopol 2011). In general, system reliability of a bridge is governed by not only the element reliability but also a number of other factors including system arrangement, correlation of element failures, post-failure behavior of elements, among others (Estes & Frangopol 1999; Zhu & Frangopol 2012; Saydam & Frangopol 2013; Barone & Frangopol 2014b; Zhu & Frangopol 2014a; Zhu & Frangopol 2014b; Zhu & Frangopol 2015).

Ideally, the system model of a structure can be classified into one of the following four categories: (a) series systems, (b) parallel systems, (c) parallel-series systems, and (d) series-parallel systems. These four types of idealized systems are schematically represented by either reliability block diagrams or fault tree models (Rausand & Arnljot 2004). Figure 14 shows schematically the examples of these four types of systems. In the following discussions, reliability block diagrams are used to represent systems whenever possible. It should be noted that the latter two system types (i.e. parallel-series and series-parallel systems) can be transformed to one another by conducting minimal cut or minimal path analyses of systems (Leemis 1995). Therefore, the failure of a system can be represented by one of the following three cases:

(a) For a series system with n components, the event of system failure (E) can be represented by

$$E \equiv \bigcup_{k=1}^{n} \left\{ g_k\left(\mathbf{x}\right) < 0 \right\} \tag{9}$$

where $g_k(\mathbf{x}) < 0$ indicates the failure of element k.

(b) For a parallel system with n components, the event of system failure can be represented by

$$E \equiv \bigcap_{k=1}^{n} \left\{ g_k\left(\mathbf{x}\right) < 0 \right\} \tag{10}$$

(c) For a series-parallel system with n minimal cut sets, each of which contains c_k elements in parallel (k = 1, 2 , … n), the event of system failure can be represented by

$$E \equiv \bigcup_{k=1}^{n} \bigcap_{j=1}^{c_k} \left\{ g_{k,j}(\mathbf{x}) < 0 \right\} \tag{11}$$

where $g_{kj}(\mathbf{x}) < 0$ indicates the failure of element j in the kth minimal cut set of the system.

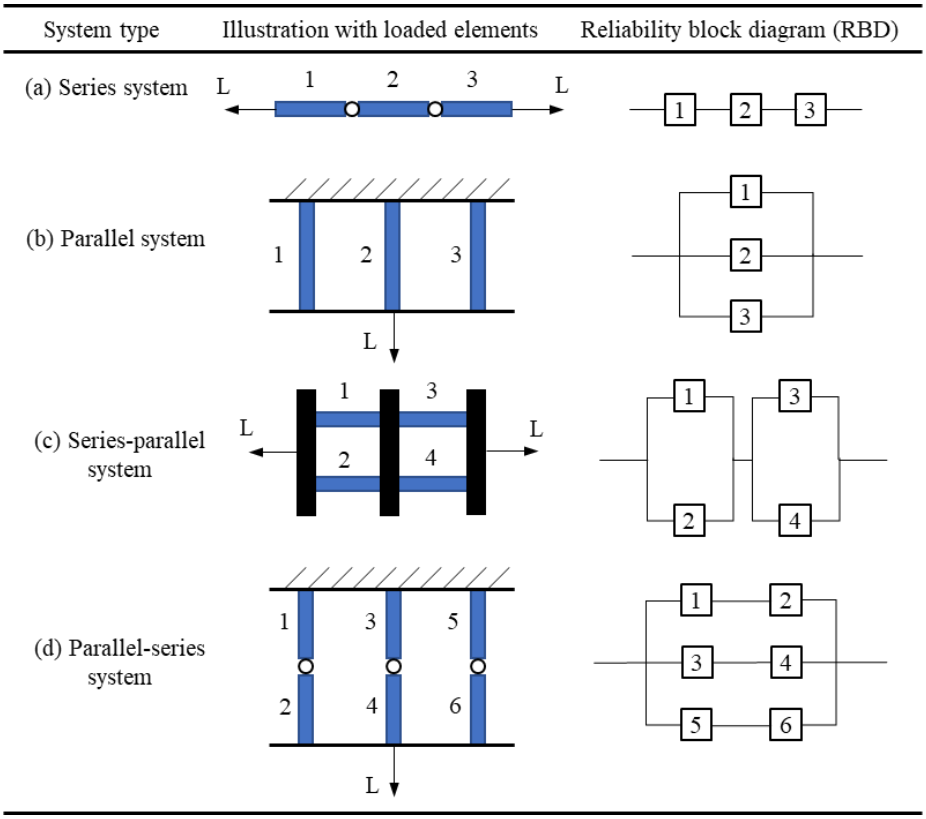

Figure 14: Idealized system models.

The system model of a bridge can be created based on the judgement and experience of bridge engineers. For instance, if reliable end and center diaphragms exist in the superstructure, parallel subsystems can be used to represent that the failure of three adjacent girders is required for the failure of the entire bridge superstructure (Estes & Frangopol 1999). As a result, the girder bridge shown in Figure 15 can be modeled as a series-parallel system considering 16 failure modes of different structural members including flexural failure of concrete deck [g(1)], shear failure of interior, exterior and interior-exterior girders (g(2), g(4), and g(6)), flexural failure of interior, exterior and interior-exterior girders [g(3), g(5), and g(7)], shear failure of pier caps [g(8)], pier cap failure under positive and negative moments [g(9) and g(10)], crushing of top columns [g(11)], crushing of bottom columns [g(12)], one-way shear failure of footing

[g(13)], two-way shear failure of footing [g(14)], flexural failure of footing [g(15)], and crushing of expansion bearing [g(16)] (Estes & Frangopol 1999). Alternatively, finite element models can be used to analyze the effects of different failure modes to system failure (Imam et al. 2012; Saydam & Frangopol 2013). For instance, Imai & Frangopol (2002) established a series-parallel system model for a suspension bridge (Honshu Shikoku Bridge, Japan) based on nonlinear finite element models.

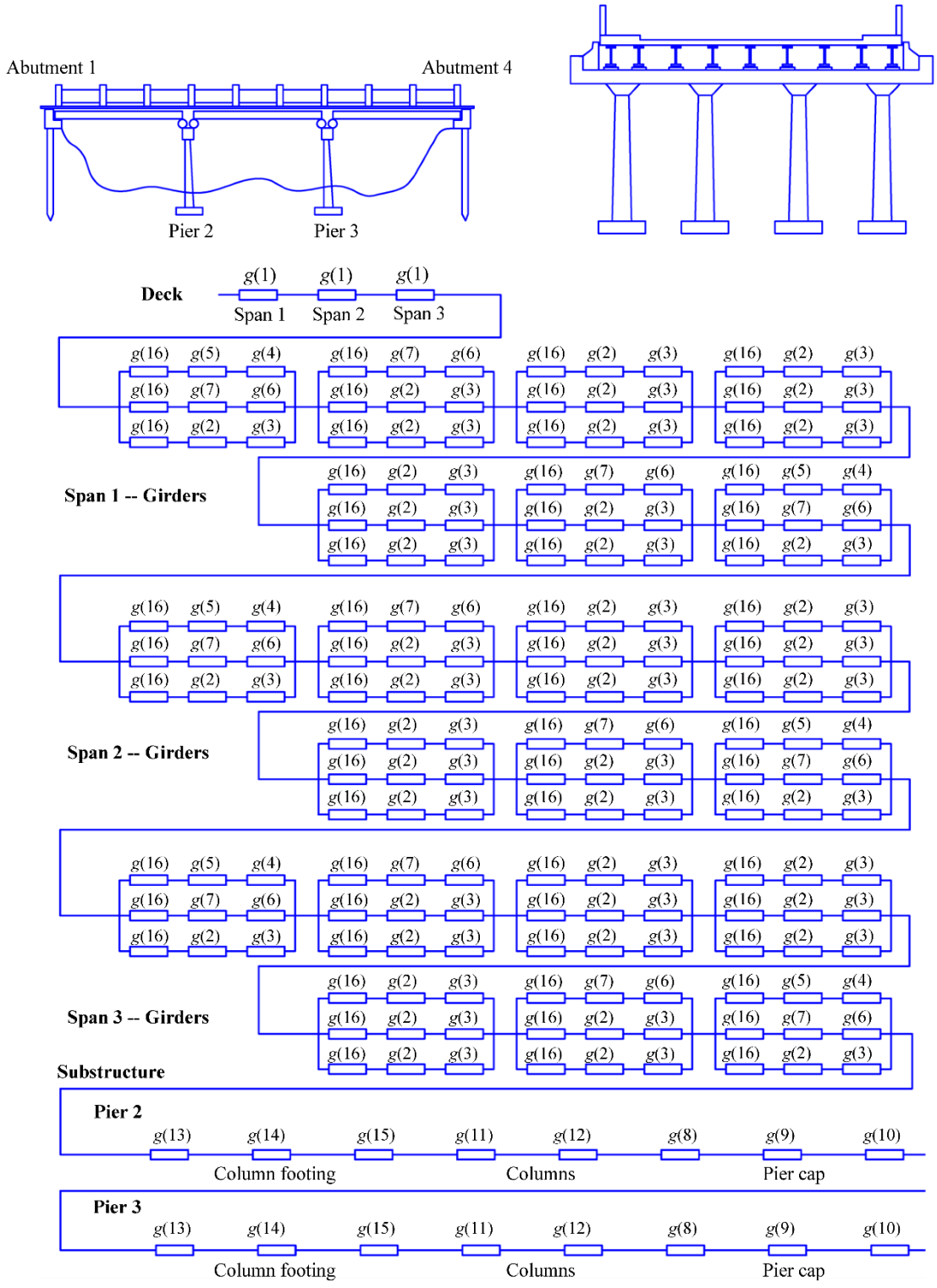

Figure 15: System model of a girder bridge [adapted from Estes & Frangopol (1999)]

Apart from defining the system model, another important factor for determining system reliability is the correlation among different failure modes (i.e. element failures) (Estes & Frangopol

1999; Zhu & Frangopol 2012). For a bridge, the load-carrying capacities of different structural members are likely to be correlated due to their similar materials and construction process. Similarly, the loading effects in the structural members are very probable to be highly correlated, especially in the case of vehicle loads where the loading effects are caused by one or a set of heavy vehicles passing the bridge and are thus nearly fully correlated. Therefore, the element failures in a bridge system are also correlated. In general, direct evaluation of correlation among random variables representing the element failure is difficult. Nevertheless, this correlation can be implicitly considered by the coefficients of correlation between random variables (*R*'s or *S*'s) in different element limit state functions. The precise evaluation of system reliability usually requires carrying out Monte Carlo simulation, which is not always viable due to the low failure probabilities of civil engineering structures. Nevertheless, the system reliability with correlated failure modes can be approximated based on the reliability bounds of series, parallel, and series-parallel systems (Estes & Frangopol 1998). Using this approach, RELSYS (RELiability of SYStems), a Fortran 77 computer program, was developed at the University of Colorado at Boulder based on the Ditlevsen bounds of system failure probabilities (Ditlevsen 1979; Estes & Frangopol 1998; Estes & Frangopol 1999). The program is currently available at the Computational Laboratory for Life-cycle Structural Engineering at Lehigh University. For systems with large numbers of elements (high dimensional problems), narrower bounds of system failure probabilities can be used to improve the quality of the approximated system reliability (Song & Der Kiureghian 2003; Song & Kang 2009). For different system models, the system reliability can be lower (as in series systems) or higher (as in parallel systems) than the element reliability. In order to obtain a consistent level of safety for different bridges, the element target reliability should be adjusted according to the system model and the correlation condition. Target reliability indices of elements in different system models and with different correlation conditions have been calculated for typical bridge system models (Zhu & Frangopol 2014b). The ultimate goal is to achieve a consistent level of reliability for different systems (e.g. the system reliability index $\beta_{sys} = 3.5$). These element target reliability indices can be used in load testing. Brittle or ductile behavior after element failure can lead to very different load redistribution paths within a system and thus affect the system reliability (Enright & Frangopol 1999). The effect of post-failure behavior has been extensively studied primarily by using event tree models (Zhu & Frangopol 2014a; Zhu & Frangopol 2015).

5 LIFE-CYCLE COST CONSIDERATIONS

As mentioned previously, the reliability of a bridge decreases in its life-cycle due to various deterioration mechanisms. Therefore, inspection, structural health monitoring, and/or timely maintenance actions must be performed to ensure structural safety in the service life (Frangopol

& Soliman 2016). All these actions will bring in additional life-cycle maintenance costs. Figure 16 shows the evolution of life-cycle performance in terms of reliability index as well as life-cycle maintenance cost under a generic deterioration process and multiple maintenance actions. In Figure 16, two types of maintenance actions are illustrated. If a maintenance action is proactive and implemented before the reliability threshold is reach, it is usually referred to as a preventative maintenance action (Frangopol et al. 1997). Alternatively, if a maintenance action is reactive as a result of the violation of a prescribed reliability threshold, such an action is called an essential maintenance action (Frangopol et al. 1997). Usually, the maintenance cost of an essential action is higher than that of a preventative action. Figure 16 shows the growth of life-cycle cost with respect to the service time. In general, the life-cycle cost of a bridge can be expressed as (Frangopol et al. 1997)

$$C_{life} = C_{ini} + \sum_{i=1}^{N_r} \frac{C_{r,i}}{(1+r)^{t_i}} + \sum_{j=1}^{N_s} \frac{C_{s,j}}{(1+r)^{t_j}} + C_{fail} \tag{12}$$

where C_{ini} is the initial cost; N_r is the number of maintenance actions; t_i and $C_{r,i}$ are the time and the cost of the ith maintenance action, respectively; N_s is the number of inspection actions; t_j and $C_{s,j}$ are the time and the cost of the jth inspection action, respectively; r is the discount rate of money; and C_{fail} is the expected failure cost.

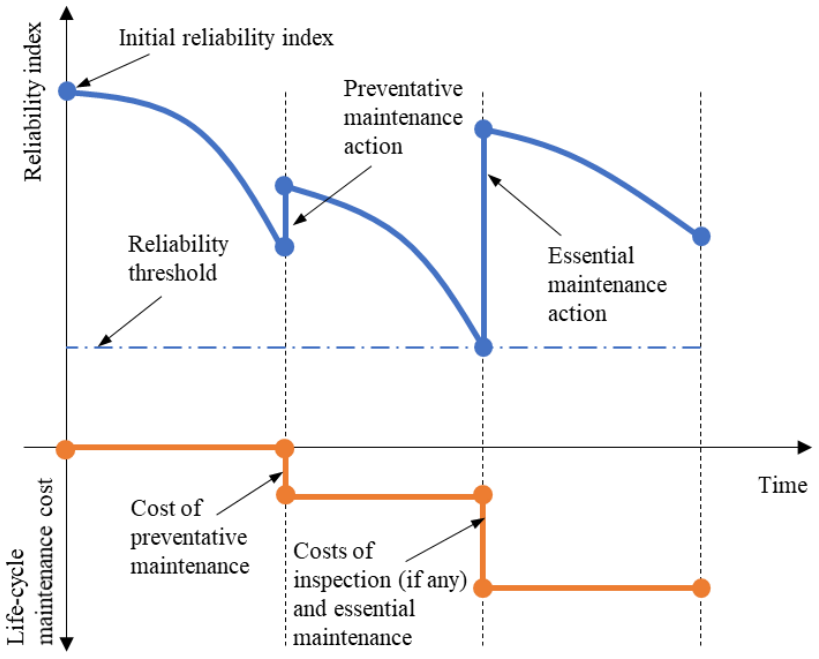

Figure 16: Life-cycle performance in terms of reliability index and the corresponding life-cycle maintenance cost.

As discussed previously in Section 2, proof load testing provides useful insight into the load-carrying capacities of bridges. In essence, load testing plays a similar role as that of an inspection action. The information obtained from load testing can be used to adjust life-cycle maintenance plans. For the two cases mentioned in Section 2, Figure 17 shows schematically the corresponding changes in essential maintenance schedules and their associated life-cycle performance and life-cycle maintenance cost. Since load testing can induce additional cost into the total life-cycle cost, the time and technique used in the testing should be optimized in the life-cycle of a bridge so that the life-cycle cost can be minimized. In Eq. (12), the initial cost C_{ini} is fixed in cases where the load testing is planned for an existing bridge. In addition, for reliability-based planning, the expected failure cost (i.e. the failure risk) can be excluded from the planning process based on the fact that the failure risk is considered tolerable as long as the reliability target is satisfied and that the decision-makers are indifferent to the further decrease of this tolerable risk. Otherwise, risk-based planning is needed. Therefore, minimization of total life-cycle cost in reliability-based load testing planning is equivalent to the minimization of life-cycle maintenance cost.

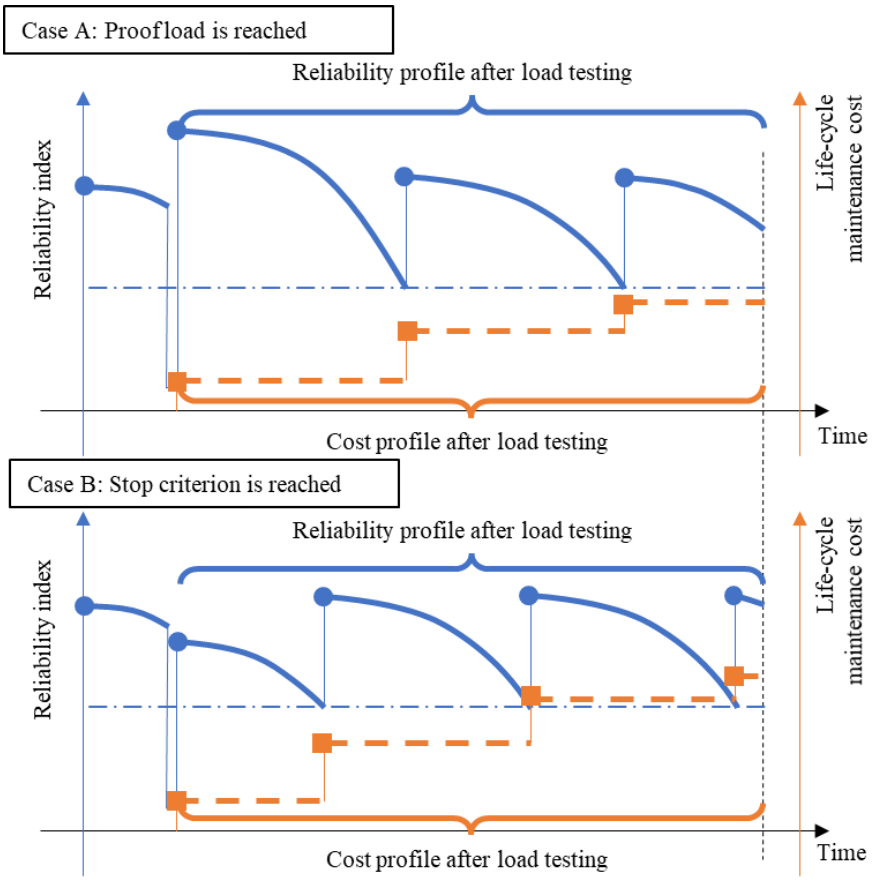

Figure 17: Life-cycle performance (in reliability index) and life-cycle maintenance cost after load testing based on different cases of testing results.

It should be noted that the occurrence of Case A (i.e. proof load is reached) or Case B (i.e. stop criterion is reached) in Figure 17 is not known a priori in the planning phase of load testing. Therefore, optimization of load testing plans must be conducted in a preposterior manner (Ang & Tang 1984). Such approaches have been used to optimize inspection plans of various civil and marine structures under different deterioration mechanisms (Kwon & Frangopol 2011; Kim & Frangopol 2012; Kim et al. 2013; Soliman et al. 2016). For load testing planning, an illustrative decision-tree model can be established as shown in Figure 18. The reliability-based load testing planning can be formulated as the following optimization problem:

Given

Bridge model, deterioration model, and models for preventative and essential maintenance actions,

Find

Time and technique of loading testing in the life-cycle of the bridge

So that

The total life-cycle cost is minimized

Subjected to

(a) that the lowest reliability index of the bridge in its life-cycle is higher than the reliability target,

(b) the budget for load testing, and

(c) the budget for maintenance actions

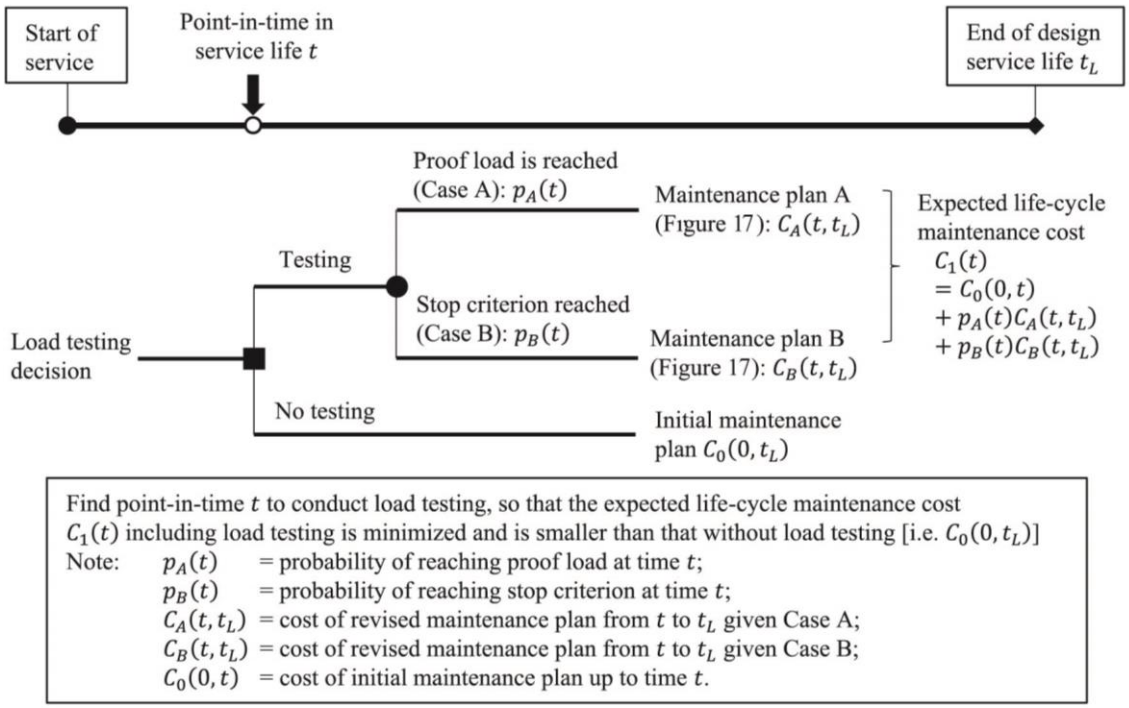

Figure 18: Decision-tree model for load testing planning.

The aforementioned reliability-based planning can be extended further to risk-based planning by considering the consequence of structural failure. Risk is herein defined as the product of failure probability and the associated failure consequences, as represented by the following equation:

$$R_f = p_f \cdot C_f \tag{13}$$

where R_f is the failure risk; p_f is the failure probability; C_f is the failure consequences. The difference between reliability-based and risk-based planning is that the former uses a reliability target to implicitly regulate the tolerable risk, while the latter explicitly calculates the risk value and treats it as a part of the optimization objective or a separate objective overall. Usually the failure consequences are measured or converted to monetary value. For a bridge structure, the consequences of bridge failure include the direct cost of reconstruction and the social cost borne by traffic users in the form of economic losses due to extra travel time and extra travel distance (Decò & Frangopol 2011).

The obtained risk value can be considered as a separate objective, thereby forming a bi-objective optimization that simultaneously minimizes the life-cycle failure risk and life-cycle maintenance cost. The results of this bi-objective problem can be presented in a Pareto front which represents the optimal compromises between these two objectives. Alternatively, the life-cycle

failure risk can be considered as failure cost and be added to the total life-cycle cost. As expected, with increasing budgets for load testing and maintenance, the failure risk is likely to be reduced. Figure 19 shows the qualitative relation between budgets and risk. It can be seen from Figure 19 that by using risk-based planning, the optimal budget for reducing total life-cycle cost can be determined.

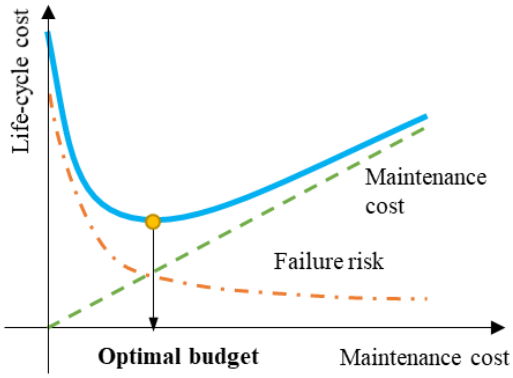

Figure 19: Determination of optimal budget for maintenance

Bridge failure can have dire impacts in economic, social, and environmental terms. Not all these consequences can be expressed in monetary value. The utilities of economic, social, and environmental impacts in the decision-making process are largely governed by the risk perceptions and risk attitudes of stakeholders. Therefore, a sustainability-informed approach for risk assessment and risk-based planning has been advocated in recent studies (Dong et al. 2013; Bocchini et al. 2014; Sabatino et al. 2015; Liu et al. 2018). García-Segura et al. (2017) showed that life-cycle maintenance plans optimized based on economic or environmental objectives can hold very different outlooks due to the different time values of economic and environmental consequences. Sabatino et al. (2016) introduced multi-attribute utility theory (MAUT) into sustainability-informed risk-based planning to (a) convert consequences of different units to a consistent utility value in the range of [0, 1] and (b) combine economic, social, and environmental consequences to a sustainability utility value based on risk attitudes of decision makers. MAUT-based frameworks for life-cycle management have been proofed to be an effective tool to harmonize the economic, social, and environmental aspects of sustainability (Dong et al. 2015; Sabatino et al. 2016; Yang & Frangopol 2018).

6 SUMMARY AND CONCLUSIONS

This chapter discusses load testing from the perspective of structural reliability. In a proof load test, the applied target proof load results in a certain load effect. If the structure can withstand the applied load without signs of distress (and the proof load test is successful), it has been

shown experimentally that the structure has a capacity that is larger than or equal to the load effect caused by the applied load. As such, the probability density function of the resistance at the considered cross-section can be truncated at the level of the load effect caused by the applied load, and the reliability index can be recalculated. Alternatively, the target proof load to demonstrate a certain reliability index can be found by applying these principles. This reliability index is lower for existing structures than for new structures. Taking into account as well the dimension of time and the effects of degradation, the optimum time for a load test can be determined.

This chapter contains two examples of proof load tests for which the target proof load was determined as a function of the target reliability index that the load test should demonstrate. For viaduct De Beek, the target proof load was determined a posteriori and for the Halvemaans Bridge, the target proof load was determined a priori. For viaduct De Beek, a flexure-critical reinforced concrete slab bridge, no traffic information is available. Recommendations from the JCSS Probabilistic Model Code are used to determine the probability density functions of the acting bending moment and the bending moment resistance. The example shows the need for recommendations on the assumptions for the coefficient of variation that can be used in simplified analyses for the determination of the target proof load when no traffic information is available. The example of the Halvemaans Bridge, a flexure-critical reinforced concrete slab bridge, shows that weigh in motion data can be used to develop a cumulative distribution function of the load effect, and how this information can be used to derive the target proof load. When traffic information is available, or can be estimated with reasonable assumptions, the presented method can be followed to determine the target proof load.

The concepts in the first half of this chapter are based on an analysis at the element level, and based on a sectional analysis. It is more realistic to consider the bridge in its entirety and calculate the systems reliability, or to even consider the bridge as part of the entire infrastructure network by determining the measures (including load testing) that should be taken during the lifecycle of the bridge to minimize the cost (economic, environmental, and social). To consider the bridge in its entirety, systems reliability considerations are required. The failure mode of the system needs to be determined by analyzing the system based on the system type (series, parallel, or a combination of series and parallel), based on judgement and experience of bridge engineers, or based on nonlinear finite element models. In principle, the correlation between failure modes (correlation of capacity for different failure modes and correlation of loading effects) should be taken into account. Such considerations require a large computation effort. When the systems reliability index is a constant and known value, depending on the structural system and

correlation between failure modes, the target reliability index of each element can be determined. The target reliability index of the elements can then be used to determine the target proof load to be used during a load test to demonstrate the required systems reliability index.

When load testing is considered from a life-cycle perspective, the goal is to minimize the life-cycle cost of the structure by including actions such as maintenance, inspections, and load testing. Depending on the outcome of a load test, the life-cycle maintenance plan of a given structure may need to be adjusted. Life-cycle cost optimization calculations can also be used to determine the optimal time during the life of a structure for a load test. This minimized cost should encompass the economic, environmental, and social cost.

REFERENCES

AASHTO 2016. *The Manual for Bridge Evaluation with 2016 Interim Revisions,* Washington, D.C.: American Association of State Highway and Transportation Officials (AASHTO).

Ang, A.H.-S. & Tang, W.H., 2007. *Probability Concepts in Engineering: Emphasis on Applications in Civil & Environmental Engineering,* Hoboken, NJ: Wiley.

Ang, A.H.-S. & Tang, W.H., 1984. *Probability Concepts in Engineering Planning and Design, Vol. 2: Decision, Risk, and Reliability*, New York, NY: Wiley.

Barone, G. & Frangopol, D.M., 2014a. Life-cycle maintenance of deteriorating structures by multi-objective optimization involving reliability, risk, availability, hazard and cost. *Structural Safety*, 48: 40–50.

Barone, G. & Frangopol, D.M., 2014b. Reliability, risk and lifetime distributions as performance indicators for life-cycle maintenance of deteriorating structures. *Reliability Engineering and System Safety*, 123: 21–37.

Bocchini, P., Frangopol, D.M., Ummenhofer, T. & Zinke, T., 2014. Resilience and sustainability of civil infrastructure: Toward a unified approach. *Journal of Infrastructure Systems, ASCE*, 20(2): 04014004.

Bocchini, P. & Frangopol, D.M., 2011. Generalized bridge network performance analysis with correlation and time-variant reliability. *Structural Safety*, 33(2): 155–164.

Bocchini, P. & Frangopol, D.M., 2012. Restoration of bridge networks after an earthquake: Multicriteria intervention optimization. *Earthquake Spectra*, 28(2): 427–455.

Bocchini, P. & Frangopol, D.M., 2013. Connectivity-based optimal scheduling for maintenance of bridge networks. *Journal of Engineering Mechanics*, 139(6): 760–769.

Casas, J.R. & Gómez, J.D., 2013. Load rating of highway bridges by proof-loading. *KSCE Journal of Civil Engineering*, 17: 556-567.

CEN 2003. *Eurocode 1: Actions on Structures - Part 2: Traffic Loads on Bridges, NEN-EN* 1991-2:2003. Brussels, Belgium: Comité Européen de Normalisation.

Code Committee 351001 2011. *Assessement of Structural Safety of an Existing Structure at Repair or Unfit for Use - Basic Requirements, NEN 8700:2011 (in Dutch)*, Delft, The Netherlands: Civil center for the execution of research and standard, Dutch Normalisation Institute.

Decò, A. & Frangopol, D.M., 2011. Risk assessment of highway bridges under multiple hazards. *Journal of Risk Research*, 14(9): 1057–1089.

Ditlevsen, O., 1979. Narrow Reliability Bounds for Structural Systems. *Journal of Structural Mechanics*, 7(4): 453–472.

Dong, Y., Frangopol, D.M. & Sabatino, S., 2015. Optimizing bridge network retrofit planning based on cost-benefit evaluation and multi-attribute utility associated with sustainability. *Earthquake Spectra*, 31(4): 2255–2280.

Dong, Y., Frangopol, D.M. & Saydam, D., 2013. Time-variant sustainability assessment of seismically vulnerable bridges subjected to multiple hazards. *Earthquake Engineering & Structural Dynamics*, 42: 1451–1467.

Enright, M. P. & Frangopol, D. M. 1998. Probabilistic analysis of resistance degradation of reinforced concrete bridge beams under corrosion. *Engineering Structures,* 20**,** 960-971.

Enright, M.P. & Frangopol, D.M., 1999. Reliability-based condition assessment of deteriorating concrete bridges considering load redistribution. *Structural Safety*, 21(2): 159–195.

Estes, A.C. & Frangopol, D.M., 1998. RELSYS: A Computer Program for Structural System Reliability. *Structural Engineering and Mechanics*, 6(8): 901–919.

Estes, A.C. & Frangopol, D.M., 1999. Repair optimization of highway bridges using system reliability approach. *Journal of Structural Engineering*, 125(7): 766–775.

Fennis, S. A. A. M. & Hordijk, D. A. 2014. Proof loading Halvemaans Bridge Alkmaar (in Dutch). Delft, The Netherlands: Delft University of Technology.

fib Task Group 3.1 2016. *Partial Factor Methods for Existing Concrete Structures*.

Frangopol, D.M., 2011. Life-cycle performance, management, and optimisation of structural systems under uncertainty: accomplishments and challenges. *Structure and Infrastructure Engineering*, 7(6): 389–413.

Frangopol, D.M., Dong, Y. & Sabatino, S., 2017. Bridge life-cycle performance and cost: analysis, prediction, optimisation and decision-making. *Structure and Infrastructure Engineering*, 13(10): 1239–1257.

Frangopol, D.M. & Kim, S., 2014. Chapter 18: Life-cycle analysis and optimization. in Chen, W.F. & Duan, L. (eds.) *Bridge Engineering Handbook, Vol. 5 Construction and Maintenance.* Boca Raton, FL: CRC Press / Taylor & Francis Group.

Frangopol, D.M., Lin, K.-Y. & Estes, A.C., 1997. Life-cycle cost design of deteriorating structures. *Journal of Structural Engineering*, 123(10): 1390–1401.

Frangopol, D.M. & Liu, M., 2007. Maintenance and management of civil infrastructure based on condition, safety, optimization, and life-cycle cost. *Structure and Infrastructure Engineering*, 3(1): 29–41.

Frangopol, D.M. & Soliman, M., 2016. Life-cycle of structural systems: recent achievements and future directions. *Structure and Infrastructure Engineering*, 12(1): 1–20.

García-Segura, T., Yepes, V., Frangopol, D.M. & Yang, D.Y., 2017. Lifetime reliability-based optimization of post-tensioned box-girder bridges. *Engineering Structures*, 145: 381–391.

Gokce, H.B., Catbas, F.N. & Frangopol, D.M. 2011. Evaluation of load rating and system reliability of movable bridge. *Transportation Research Record*, 2251: 114-122.

Imai, K. & Frangopol, D.M., 2002. System reliability of suspension bridges. *Structural Safety*, 24(2–4): 219–259.

Imam, B.M., Chryssanthopoulos, M.K. & Frangopol, D.M., 2012. Fatigue system reliability analysis of riveted railway bridge connections. *Structure and Infrastructure Engineering*, 8(10): 967–984.

ISO/TC 98/SC 2 Reliability of Structures 2015. ISO 2394:2015 General principles on reliability for structures. International Organization for Standardization.

JCSS 2001a. *JCSS Probabilistic Model Code - Part 3: Resistance Models*. Joint Committee On Structural Safety (JCSS).

JCSS 2001b. *JCSS Probabilistic Model Code - Part 2: Load Models*. Joint Committee On Structural Safety (JCSS).

Karmazinova, M. & Melcher, J., 2012. Influence of steel yield strength value on structural reliability. *Recent Researches in Environmental and Geological Sciences*, 441-446.

Kim, S. & Frangopol, D.M., 2012. Probabilistic bicriterion optimum inspection/monitoring planning: applications to naval ships and bridges under fatigue. *Structure and Infrastructure Engineering*, 8(10): 912–927.

Kim, S. & Frangopol, D.M., 2017. Efficient multi-objective optimisation of probabilistic service life management. *Structure and Infrastructure Engineering*, 13(1): 147–159.

Kim, S., Frangopol, D.M. & Soliman, M., 2013. Generalized probabilistic framework for optimum inspection and maintenance planning. *Journal of Structural Engineering, ASCE*, 139: 435–447.

Koteš, P. & Vican, J., 2013. Recommended reliability levels for the evaluation of existing bridges according to eurocodes. *Structural Engineering International*, 23: 411-417.

Kwon, K. & Frangopol, D.M., 2011. Bridge fatigue assessment and management using reliability-based crack growth and probability of detection models. *Probabilistic Engineering Mechanics*, 26(3): 471–480.

Lantsoght, E., Koekkoek, R., Yang, Y., Van Der Veen , C., Hordijk, D. & De Boer, A., 2017a. Proof load testing of the viaduct De Beek. *39th IABSE Symposium - Engineering the Future.* Vancouver, Canada.

Lantsoght, E. O. L., Koekkoek, R. T., Veen, C. V. D., Hordijk, D. A. & Boer, A. D. 2017b. Pilot proof-load test on viaduct de beek: Case study. *Journal of Bridge Engineering*, 22: 05017014.

Lantsoght, E. O. L., Van Der Veen, C., De Boer, A. & Hordijk, D. A., 2017c. Required proof load magnitude for probabilistic field assessment of viaduct De Beek. *Engineering Structures*, 148: 767-779.

Lantsoght, E. O. L., Van Der Veen, C., Hordijk, D. A. & De Boer, A., 2017d. Reliability index after proof load testing: viaduct De Beek. *ESREL 2017*. Protoroz, Slovenia.

Leemis, L.M., 1995. *Reliability: probabilistic models and statistical methods*, Upper Saddle River, NJ, USA: Prentice-Hall, Inc.

Li, C. Q., Lawanwisut, W. & Zheng, J. J. 2005. Time-dependent reliability method to assess the serviceability of corrosion-affected concrete structures. *Journal of Structural Engineering-Asce*, 131: 1674-1680.

Liu, L., Frangopol, D.M., Mondoro, A. & Yang, D.Y., 2018. Sustainability-informed bridge ranking under scour based on transportation network performance and multi-attribute utility. *Journal of Bridge Engineering, ASCE* (in press).

Liu, M. & Frangopol, D.M., 2005. Time-dependent bridge network reliability: novel approach. *Journal of Structural Engineering*, 131(2): 329–337.

Liu, M. & Frangopol, D.M., 2006a. Optimizing bridge network maintenance management under uncertainty with conflicting criteria: Life-cycle maintenance, failure, and user costs. *Journal of Structural Engineering*, 132(11): 1835–1845.

Liu, M. & Frangopol, D.M., 2006b. Probability-based bridge network performance evaluation. *Journal of Bridge Engineering*, 11(5): 633–641.

Lukic, M. & Cremona, C., 2001. Probabilistic assessment of welded joints versus fatigue and fracture. *Journal of Structural Engineering-ASCE,* 127: 211-218.

Melchers, R.E. 1999. *Structural Reliability: Analysis and Prediction*. Chichester: John Wiley.

Messervey, T.B., 2009. *Integration of Structural Health Monitoring into the Design, Assessment, and Management of Civil Infrastructure*. Università di Pavia.

Messervey, T.B. & Frangopol, D.M., 2008. Innovative treatment of monitoring data for reliability-based structural assessment. In H.-M. Koh & D. M. Frangopol, eds. *Proceedings of the Fourth International Conference on Bridge Maintenance, Safety, and Management, IABMAS'08*. Seoul, Korea: CRC Press/Balkema, Taylor & Francis Group, 1466–1474.

Messervey, T.B., Frangopol, D.M. & Casciati, S., 2011. Application of the statistics of extremes to the reliability assessment and performance prediction of monitored highway bridges. *Structure and Infrastructure Engineering*, 7(1): 87–99.

NCHRP 1998. *Manual for Bridge Rating through Load Testing*. Washington, DC.

Obrien, E. J., Schmidt, F., Hajializadeh, D., Zhou, X. Y., Enright, B., Caprani, C. C., Wilson, S. & Sheils, E. 2015. A review of probabilistic methods of assessment of load effects in bridges. *Structural Safety,* 53**,** 44-56.

Okasha, N.M. & Frangopol, D.M., 2009. Lifetime-oriented multi-objective optimization of structural maintenance considering system reliability, redundancy and life-cycle cost using GA. *Structural Safety*, 31(6): 460–474.

Olaszek, P., Świt, G. & Casas, J. R. 2012. Proof load testing supported by acoustic emission. An example of application. *IABMAS 2012*.

Rausand, M. & Arnljot, H.Ã., 2004. *System Reliability Theory: Models, Statistical Methods, and Applications* , 2nd ed., John Wiley & Sons.

Righiniotis, T. D. & Chryssanthopoulos, M. K. 2003. Probabilistic fatigue analysis under constant amplitude loading. *Journal of Constructional Steel Research,* 59**,** 867-886.

Rijkswaterstaat 2013. *Guidelines Assessment Bridges - Assessment of Structural Safety of an Existing Bridge at Reconstruction, Usage and Disapproval* (in Dutch), RTD 1006:2013 1.1.

Sabatino, S., Frangopol, D.M. & Dong, Y., 2015. Sustainability-informed maintenance optimization of highway bridges considering multi-attribute utility and risk attitude. *Engineering Structures*, 102: 310–321.

Sabatino, S., Frangopol, D.M. & Dong, Y., 2016. Life cycle utility-informed maintenance planning based on lifetime functions: optimum balancing of cost, failure consequences and performance benefit. *Structure and Infrastructure Engineering*, 12(7): 830–847.

Šavor, Z. & Šavor Novak, M. 2015. Procedures for reliability assessment of existing bridge. *Građevinar,* 67**,** 557-572.

Saydam, D. & Frangopol, D.M., 2013. Applicability of simple expressions for bridge system reliability assessment. *Computers and Structures*, 114–115: 59–71.

Soliman, M., Frangopol, D.M. & Mondoro, A., 2016. A probabilistic approach for optimizing inspection, monitoring, and maintenance actions against fatigue of critical ship details. *Structural Safety*, 60: 91–101.

Song, J. & Kang, W.H., 2009. System reliability and sensitivity under statistical dependence by matrix-based system reliability method. *Structural Safety*, 31(2): 148–156.

Song, J. & Der Kiureghian, A., 2003. Bounds on System Reliability by Linear Programming. *Journal of Engineering Mechanics*, 129(6): 627–636.

Spaethe, G. 1994. The effect of proof load testing on the safety of a structure (in German). *Bauingenieur,* 69**,** 459-468.

Steenbergen, R. D. J. M. & Vrouwenvelder, A. C. W. M. 2010. Safety philosophy for existing structures and partial factors for traffic loads on bridges. *Heron,* 55: 123-140.

Stewart, M. G., Rosowsky, D. V. & Val, D. V. 2001. Reliability-based bridge assessment using risk-ranking decision analysis. *Structural Safety,* 23: 397-405.

Vatteri, A. P., Balaji Rao, K. & Bharathan, A. M. 2016. Time-variant reliability analysis of RC bridge girders subjected to corrosion – shear limit state. *Structural Concrete,* 17**,** 162-174.

Willems, M., Ruiter, P. B. D. & Heystek, A. P. 2015. *Inspection Report Object* 51H-304-01 (in Dutch).

Yang, D.Y. & Frangopol, D.M., 2018. Bridging the gap between sustainability and resilience of civil infrastructure using lifetime resilience. In P. Gardoni, ed. *Handbook of Sustainable and Resilient Infrastructure*. Routledge, (in press).

Zhu, B. & Frangopol, D.M., 2012. Reliability, redundancy and risk as performance indicators of structural systems during their life-cycle. *Engineering Structures*, 41: 34–49.

Zhu, B. & Frangopol, D.M., 2013. Incorporation of structural health monitoring data on load effects in the reliability and redundancy assessment of ship cross-sections using Bayesian updating. *Structural Health Monitoring-an International Journal*, 12: 377-392.

Zhu, B. & Frangopol, D.M., 2014a. Effects of postfailure material behavior on system reliability. *ASCE-ASME Journal of Risk and Uncertainty in Engineering Systems, Part A: Civil Engineering*, 1(1): 04014002.

Zhu, B. & Frangopol, D.M., 2014b. Redundancy-based design of nondeterministic systems. In D. M. Frangopol & Y. Tsompanakis, eds. *Maintenance and Safety of Aging Infrastructure in the Book Series Structures and Infrastructures*. London: CRC Press/Balkema, Taylor & Francis Group, 707–738.

Zhu, B. & Frangopol, D.M., 2015. Effects of post-failure material behaviour on redundancy factor for design of structural components in nondeterministic systems. *Structure and Infrastructure Engineering*, 11(4): 466–485.